

Concentration inhomogeneities in random magnets. I. Characterization using optical birefringence

A. R. King, I. B. Ferreira, and V. Jaccarino

Department of Physics, University of California, Santa Barbara, California 93106

D. P. Belanger

Department of Physics, University of California, Santa Cruz, California 95064

(Received 9 March 1987)

The optical birefringence technique is used to precisely characterize the macroscopic concentration gradients that invariably arise in the growth of two-component, optically anisotropic, single crystals from the melt. The method is nondestructive, volumetric, and performable at ambient temperatures. Particular application is made to the $\text{Fe}_x\text{Zn}_{1-x}\text{F}_2$ system because of the extensive studies that have been made on this diluted Ising antiferromagnet in connection with the random-exchange and random-field Ising-model problems. Variations of the observed gradient appear to be related to factors involved in the solidification process. Through use of this technique means are obtained for choosing between crystal-growth methods, selecting the best regions of a crystal, and for developing criteria for the selection (or rejection) of any given one, for critical-phenomena studies.

I. INTRODUCTION

There has been an increasing interest in the physics of random systems from both the theoretical and experimental points of view. However, the presumption of quenched disorder on all length scales, tacitly assumed in most theories of the properties of random systems, is virtually never realized in practice. Departures from a perfectly random distribution of the atomic components in the preparation of a binary system occur for a variety of reasons (clustering, segregation of phases, differential solid solubility at the liquid-solid interface, etc.). Whatever the reasons, it is important to be able to precisely characterize the inhomogeneity, whether it be of microscopic or macroscopic origin so that account may be taken of it in the comparisons of experimental measurements with theories of random systems.

One particular type of nonrandomness is produced by the concentration gradient that invariably arises in the growth from the melt of single crystals of a pseudo-binary system (e.g., $\text{Fe}_x\text{Zn}_{1-x}\text{F}_2$). For a small, but finite size crystal of, say, 50 mm^3 , the presence of a fractional concentration variation along the crystal growth direction of as little as $\delta x/x \simeq 10^{-2}$ might present no problems in the interpretation of the low-temperature phonon or magnon dispersion. However, in studies of the critical behavior of random systems, a concentration gradient even as small as this might result in erroneous values being obtained for the critical exponents and amplitude ratios from analyses of the various thermodynamic properties at the phase transition. This is a consequence of the variation of T_c with x along the gradient direction. Close to T_c a small variation in T_c pro-

duces a relatively large variation in the reduced temperature $|t| \equiv |1 - T/T_c|$, and thereby limits the range of t over which a meaningful interpretation of critical phenomena can be made.

It is with this latter concern in mind that we have sought to develop a method which would provide an accurate characterization of the concentration gradient in the mixed or randomly diluted transition-metal difluorides. The technique we have employed is linear optical birefringence. Although the method is nondestructive and is readily performed at ambient temperatures, it does have some obvious limitations. The crystals of interest must be reasonably transparent somewhere in the visible region, and they obviously have to be optically anisotropic; hence mixed cubic crystals cannot be probed with this technique.

II. EXPERIMENTAL METHOD

An apparatus has been developed and used for the past five years to make precision measurements of the optical linear birefringence Δn , using a variation of the Senarmont technique. It has been described in detail elsewhere¹ but, suffice it to say, it is capable of measuring changes in Δn as small as $\delta(\Delta n) \sim 10^{-8}$ in a 4-mm-thick crystal. This inherent sensitivity of the technique has been exploited in critical-phenomena studies of both pure (e.g., Rb_2CoF_4) and randomly diluted (e.g., $\text{Fe}_x\text{Zn}_{1-x}\text{F}_2$) systems,²⁻⁶ by measuring the temperature dependence of the derivative of the magnetic birefringence $d(\Delta n)_m/dT$.

In the context of the work to be described below, the same apparatus has been used as a means for measuring

the *spatial* variation of Δn , at a fixed *ambient* temperature, in a two-component single crystal with presumed quenched randomness. This variation in Δn (if it exists) is then used to characterize the macroscopic inhomogeneity in the relative concentration of the two components of the mixed system (e.g., FeF_2 and ZnF_2 in $\text{Fe}_x\text{Zn}_{1-x}\text{F}_2$). The birefringence analysis of the concentration gradient requires that two carefully polished sides be prepared on opposite sides of the crystal, with the faces kept parallel to a few parts in 10^4 . This is accomplished by standard optical polishing techniques.

The sensitivity of the Senarmont method can be understood by considering the magnitude of the angle θ by which the initial polarization has rotated in the apparatus in traversing a crystal of thickness t with birefringence Δn ,

$$\theta = \pi \Delta n t / \lambda, \quad (1)$$

where λ is the wavelength of light. We see from Eq. (1) that for a fixed average x and fixed t , a concentration variation δx can be obtained from the change in polarization angle $\delta\theta$,

$$\delta x = \lambda / \pi t [d(\Delta n)/dx]_x^{-1} \delta\theta, \quad (2)$$

where the quantity $[d(\Delta n)/dx]_x$ may be a function of x . An angular resolution of 10^{-2} deg $\simeq 2 \times 10^{-4}$ rad is obtainable with the Senarmont method. Since $t/\lambda \sim 10^4$ and $[d(\Delta n)/dx]^{-1} \simeq 10^2$ in $\text{Fe}_x\text{Zn}_{1-x}\text{F}_2$, one could, in principle, measure variations in x of order 10^{-6} .

Making a one-to-one correspondence between spatial variations in Δn and relative concentration, however, requires a calibration first be obtained of $d(\Delta n)/dx$, and hence the *absolute* value of Δn versus x for the particular two-component system under investigation. With Δn typically of order 10^{-2} a sample thickness of a few millimeters will cause a rotation of the polarization angle of order 100π . Such a large angular change makes an *absolute* determination of Δn difficult using the Senarmont technique, although relative changes of 10^{-8} are readily measurable. Instead, we resort to a more standard laboratory technique for separately measuring the ordinary (n_o) and extraordinary (n_e) indices of refraction at several values of x , and in so doing obtain $\Delta n \equiv n_e - n_o$ versus x .

Since many mixed crystals already existed upon which Δn experiments had been made, and the average concentration \bar{x} determined from measurements of T_N , it was desirable to measure n_e and n_o on these same samples. Unfortunately, the *standard* minimum-deviation-angle prism method⁷ was unsuitable in this case since the samples were rectangular and, therefore, beyond the cutoff angle for total internal reflection. However, by imbedding the crystals between glass prisms with index-matching oil, total internal reflection is prevented; see Fig. 1. In the Appendix it is shown that sample indices are given in terms of the minimum deviation angle for θ_m for this geometry by

$$n_2 = \sin(\theta_m/2) + [n_1^2 - \sin^2(\theta_m/2)]^{1/2}. \quad (3)$$

Using this technique we have measured n_o and n_e

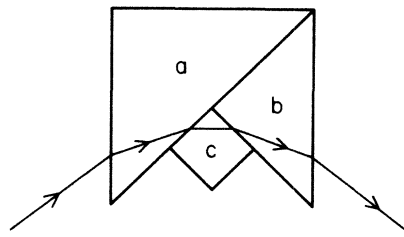


FIG. 1. Experimental configuration used to measure indices of refraction. Light rays are indicated by arrowed segments. Between crystal (c) and prisms (a and b) is an index-matching oil to prevent total internal reflection. See the Appendix for details.

with a standard laboratory spectroscope at $\lambda = 632.8$ nm as a function of x . These are shown in Fig. 2 along with Δn versus x for the $\text{Fe}_x\text{Zn}_{1-x}\text{F}_2$ system. The measurements of pure FeF_2 and ZnF_2 agree with earlier studies of Jahn⁸ to within $\sim 10^{-3}$. Most of the variation in the indices with x occurs in n_o . Also note Δn does not vary linearly with x , a consequence of which is that the instantaneous slope $[d(\Delta n)/dx]_x$ must be used for accurate determination of the relation between variations in Δn and those in concentration, at a particular value of x . To our knowledge, no theories exist for the *variation* of the birefringence in mixed crystals.

Since the scans of the crystals to determine concentration gradients are made with the laser beam traversing the sample, the measurements are sensitive only to the concentration averaged along the length of the beam. No information is obtained about the variation of x

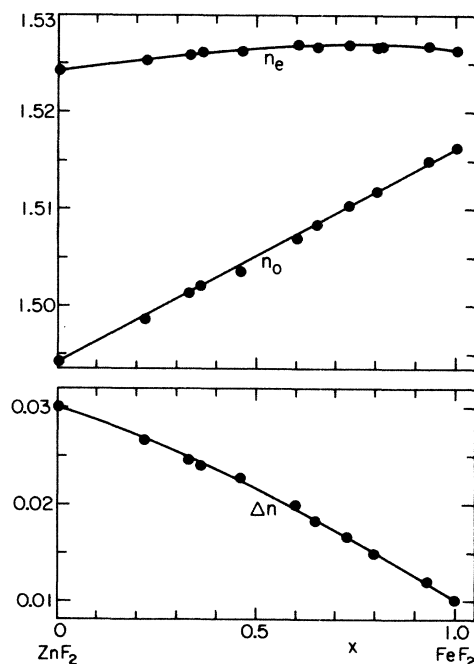


FIG. 2. Ordinary (n_o) and extraordinary (n_e) indices of refraction vs concentration for the mixed single-crystal system $\text{Fe}_x\text{Zn}_{1-x}\text{F}_2$ are shown in the upper part of figure. Solid dots are the experimental measurements at ambient temperature and the solid lines are guides to the eye. The lower part shows $\Delta n \equiv n_e - n_o$ with data obtained from the upper part of figure.

along the beam path; only the variation of the average concentration is measured in a scan. This limitation is not as serious as it might seem, as we shall see below.

III. EXAMPLES OF CONCENTRATION GRADIENT MEASUREMENTS

The $\text{Fe}_x\text{Zn}_{1-x}\text{F}_2$ crystals studied in this work were grown in the University of California, Santa Barbara (UCSB), Physics Department Materials Preparation Laboratory using variations on the stationary solidification modification to the Bridgmann-Stockbarger⁹ technique. Using appropriately oriented seed crystals, single-crystal boules were produced with the c axis either parallel or perpendicular to the growth direction. Initially, crystals were grown from the melt without any attempt at stirring or crucible rotation. However, when subsequently analyzed with the birefringence technique, several were found to exhibit large concentration gradients. In an attempt to remedy this situation, bidirectional accelerated crucible rotation (ACR) was tried since this technique is claimed to help homogenize the composition of mixed crystals grown from the melt.¹⁰ The results obtained on crystals grown by either bidirectional or unidirectional ACR proved to be equally unsatisfactory as will be discussed later on.

The most satisfactory mixed crystals were those grown using a unidirectional *constant* rotation speed of ~ 100 rev/min, which was the maximum speed in both of the ACR procedures. Although the mosaic spread has not been directly measured, it is so small that magnetic Bragg scattering by neutrons is severely extinction limited.

The polished faces must be perpendicular to the c planes if the laser beam is to simultaneously enter perpendicular to the face, and to the c axis. The crystal is mounted on an X - Y precision translator so as to be able to move the crystal in the plane perpendicular to the laser beam. A $175\text{-}\mu\text{m}$ (0.007-in.) pinhole is used to define the area to be probed. A schematic illustration of the scanning arrangement is shown in Fig. 3.

In the case of a crystal grown by solidification from the melt along a boule (z) axis, it is reasonable to expect that the liquid-solid interface should be relatively flat. Thus the gradient would be primarily along the boule axis, with transverse gradients much smaller in magnitude, and with the symmetry of the boule (e.g., cylindrical). A scan along the length of the boule would average over the small radial gradient, which we expect to be nearly independent of z , and thus accurately reflect the z gradient.

Transverse scans have been made both by the technique indicated in Fig. 3, by scanning the beam across the crystal (y scan), and also by cutting a section of the boule and scanning across it with the laser beam parallel to the boule axis. The former method has the disadvantage in that the boule cannot be scanned over its entire width, but only over the width of the polished faces. The latter method allows scanning across the full boule width, so edge effects can be seen. However, since the beam is parallel to the growth direction, we measure the transverse variation of the concentration averaged along

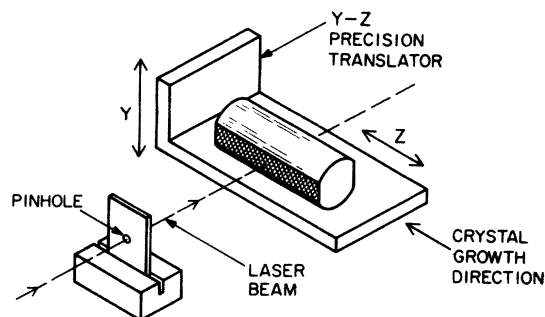


FIG. 3. Schematic of mechanical arrangement for scanning the variation of birefringence (Δn) in a mixed single crystal. The area being scanned is defined by the pinhole collimator. The crosshatched area indicates one of the two polished, parallel faces through which the laser beam passes. The top and bottom section of the original ~ 9 -mm-diam boules have been removed (see text). The z direction is chosen to be the crystal-growth direction for the following three figures.

z . We must assume that the transverse variation does not change along the boule length. The analyses that have been made of some of the crystals of $\text{Fe}_x\text{Zn}_{1-x}\text{F}_2$ using the birefringence technique are shown in Figs. 4–7. The ordinate axes are calibrated in “steps” which refer to the stepper motor used to bring the polarization analyzer to a null; one step equals a 0.01042 degree rotation of the analyzer.¹ The zero in the step number is arbitrary. Scans were usually made both *along* and *perpendicular* to the crystal-growth direction, designated as z and y , respectively. There are similarities and differences between the observed gradients in the various crystals that were studied. The most obvious common feature is that the *average* gradient is much larger parallel, than it is perpendicular, to the growth direction, as expected. In the examples shown the gradients differ in the two directions by an order of magnitude, with the *average* gradient along the growth direction varying between 0.5% to 1% per cm. However, it should be noted that gradients 10 times larger than this range quite often exist near the top and bottom of the boule. Hence the sections shown have had those portions removed. Even so, we found examples which exhibited gradients 3–5 times the average of those shown, some at the center part of the boule.

Superimposed on the approximately monotonic variation in the concentration are small scale fluctuations along the growth directions. An almost oscillatory behavior is observed in some crystals and is quite probably caused by the phenomena of “constitutional supercooling.”⁹ The most erratic variations are believed to result from poor temperature control in the solidification process and have been lessened by subsequent improvements in the crystal-growing apparatus.

In connection with the scans made perpendicular to the growth direction, there is a clear cylindrical symmetry observed in the concentration variation when any stirring or rotation method is employed. If the full diameter of the boule is scanned in this direction, the variation of the gradient is small except at the edges of the boule, presumably because of the discontinuity in heat

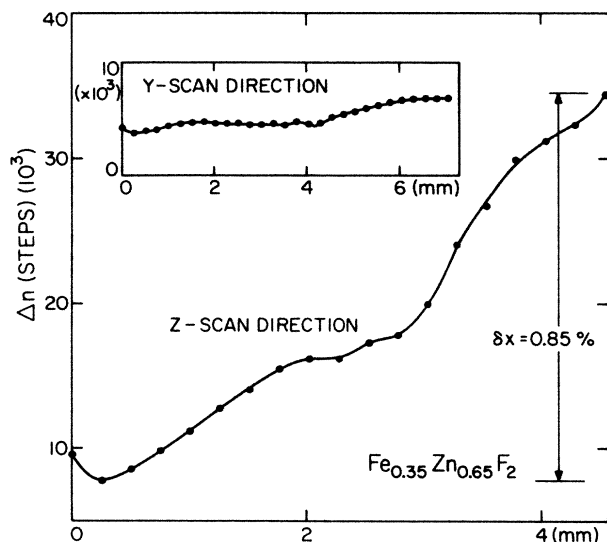


FIG. 4. Variation of Δn with distance along (z) and perpendicular (y) to the growth direction in a $\text{Fe}_{0.35}\text{Zn}_{0.65}\text{F}_2$ crystal. Using the known thickness and Eq. (2) this z -scan variation translates into a concentration variation of $\delta x = 0.85\%$. This crystal was not stirred or rotated during its growth from the melt. The y scans in Figs. 4–7 are approximately centered on the cylindrical axes of the original boules.

transport at the crucible-crystal interface.¹¹ This can be seen clearly in Figs. 6 and 7.

A particularly interesting concentration variation occurred in the growth of a nominally $\text{Fe}_{0.5}\text{Zn}_{0.5}\text{F}_2$ (actual $\text{Fe}_{0.46}\text{Zn}_{0.54}\text{F}_2$). The birefringence scan along the growth direction is shown in Fig. 7. In this instance the seed crystal was oriented with the c axis perpendicular to the growth direction. Notice that the gradient reverses itself in the middle to the crystal. Because the gradient changed sign there was a region of approximately 2 mm length (as indicated by the dashed box in Fig. 7) in

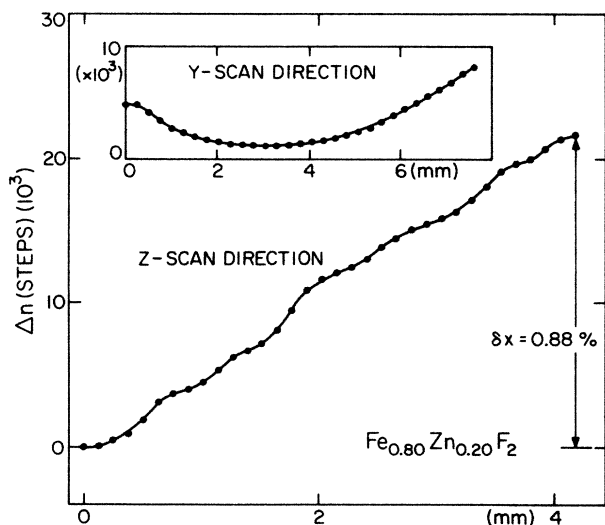


FIG. 5. Variation of Δn with distance along (z) and perpendicular (y) to growth direction in a $\text{Fe}_{0.80}\text{Zn}_{0.20}\text{F}_2$ crystal. This crystal was not rotated during its growth from the melt.

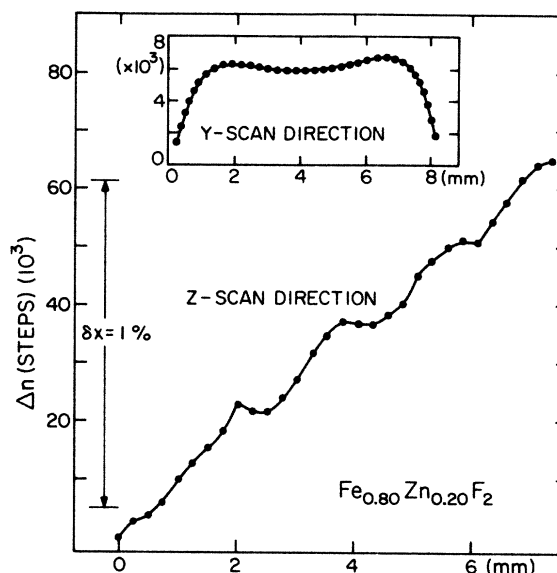


FIG. 6. Variation of Δn with distance parallel (z) and perpendicular (y) to growth direction in a $\text{Fe}_{0.80}\text{Zn}_{0.20}\text{F}_2$ crystal different from that of Fig. 5. Here the crystal was rotated at a constant velocity during its growth from the melt. Note the scale changes in comparing the two figures. The y scans in Figs. 6 and 7 are made with the laser beam parallel to the z axis and cover nearly the entire boule diameter. Note the symmetry in the radial variation of Δn shown in the text. Large changes at the edges of the boule are the results of genuine radial gradients and polishings effects.

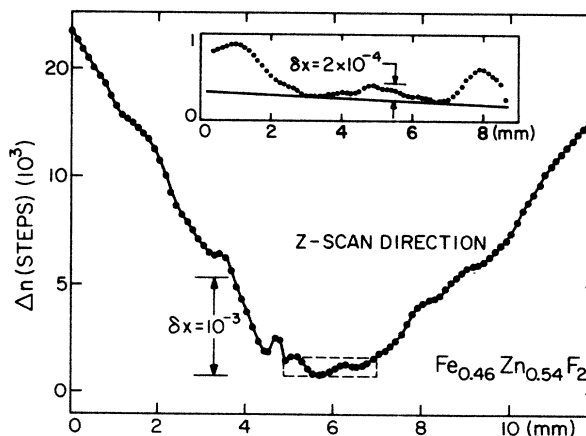


FIG. 7. Variation of Δn with distance parallel (z) to growth direction in a $\text{Fe}_{0.46}\text{Zn}_{0.54}\text{F}_2$ crystal. Note change of scales from other figures. The central portion of this crystal indicated by the dashed box was subsequently chosen for high precision critical phenomena measurements because it had a concentration spread of less than $\delta x = 2 \times 10^{-4}$ (see Refs. 12–14). The y scan is made over the central portion. The variation of Δn because of the slightly wedged shape to this section is indicated by the solid line in the inset. See also comments in the caption to Fig. 6.

which the variation in concentration $\delta x \simeq 2 \times 10^{-4}$. This section was removed from the boule, and was scanned in a direction perpendicular to the growth direction to determine the perpendicular gradient. This was found to have radial symmetry with a variation roughly twice the longitudinal variation. This select section has become the "supercrystal" upon which several recent *precision* studies of the random-exchange and random-field Ising models have either been made or are in the process of being made.¹²⁻¹⁴

Despite considerable efforts to improve upon the homogeneity of the mixed $\text{Fe}_x\text{Zn}_{1-x}\text{F}_2$ crystal no fool-proof method has been developed in our laboratory to precisely reproduce the results obtained on a given crystal when growing its successor. Although some improvements in the crystal-growth apparatus have been made, the greatest progress has been achieved through the careful selection of optimal sections of a particular crystal, and in the outright rejection of poor crystals, as judged by the Δn technique analysis.

IV. LIMITATIONS OF THE METHOD

In addition to the obvious limitation in the application of the method to crystals that are birefringent, there are other restrictive aspects to be considered. We enumerate and discuss some of the problems we have encountered in the course of studying the $\text{Fe}_x\text{Zn}_{1-x}\text{F}_2$ and related systems.

First, it is important that the difference in birefringence of the two *pure* systems be appreciable. Second, since the polarization rotation θ [Eq. (1)] is sensitive to both Δn and t , it is essential that the variation in t not outweigh the effect of interest, i.e., the Δn variation. To see how these two compare, we write

$$\delta\theta = \frac{\partial\theta}{\partial\Delta n} \frac{d\Delta n}{dx} \delta x + \frac{\partial\theta}{\partial t} \delta t \quad (4)$$

and require the first term to be larger than the second. From this we obtain, using Eq. (1),

$$\delta x > \Delta n \frac{\delta t/t}{d\Delta n/dx} \quad (5)$$

to be the minimal variation in x which is not obscured by a thickness variation δt . For example, in $\text{Fe}_{0.5}\text{Zn}_{0.5}\text{F}_2$, using $\Delta n(\text{ZnF}_2) \simeq 0.03$ and $\Delta n(\text{FeF}_2) \simeq 0.01$, we have $\Delta n \simeq 0.02$, and $d(\Delta n)/dx \sim 0.02$. With reasonable care, one can achieve a parallelism between the polished sample faces of $\delta t/t \simeq 10^{-4}$. Under these conditions the minimal $\delta x \simeq 10^{-4}$. This means that concentration gradients of $\sim 0.1\%$ over a sample can be easily determined with only a 10% error due to thickness variations. We observe here that the limitation in the measurement of δx due to the inherent resolution [Eq. (2)] is very much less than that due to the thickness variation. Thus we can accurately measure changes much smaller than $\delta x \sim 10^{-4}$ over short length scales, where t variations are proportionately smaller than $\delta t/t \sim 10^{-4}$.

However, for $\text{Mn}_x\text{Zn}_{1-x}\text{F}_2$, $d\Delta n/dx$ is expected to be some 30 times smaller than in $\text{Fe}_x\text{Zn}_{1-x}\text{F}_2$, since

$$[\Delta n(\text{ZnF}_2) - \Delta n(\text{MnF}_2)] \simeq \frac{1}{30} [\Delta n(\text{ZnF}_2) - \Delta n(\text{FeF}_2)].^8$$

In view of the extraordinary sensitivity of the Δn technique this would not rule out, *a priori*, gradient concentration determination in the $\text{Mn}_x\text{Zn}_{1-x}\text{F}_2$ system, but it would require that the thickness t versus distance along the gradient direction be determined to a 30 times greater accuracy than is necessary for the $\text{Fe}_x\text{Zn}_{1-x}\text{F}_2$ system. Alloys of the rutile transition-metal fluorides MnF_2 , FeF_2 , CoF_2 , and NiF_2 , with each other or with ZnF_2 , correspond to situations which are intermediate between the $\text{Fe}_x\text{Zn}_{1-x}\text{F}_2$ and $\text{Mn}_x\text{Zn}_{1-x}\text{F}_2$ extremes, as to differences in Δn of the respective two pure systems. Hence in all of these mixed systems, accurate concentration gradient characterization by the Δn technique should be possible provided some special care is exercised as to the parallelism of the faces along the direction in which the scan is to be made.

Two closely related considerations are the optical transparency and optical quality of a given crystal or alloy system. Clearly, a metallic crystal or one with very strong optical absorptions throughout the visible region could not be probed with this technique. However, the Senarmont *null* technique is insensitive to any effects associated with small absorptions or light intensity fluctuations. (At HeNe laser wavelengths the transition-metal fluorides discussed have very small absorptions.) However, even if the mixed crystal is transparent, it may be of such poor optical quality that birefringence studies to characterize the gradient become virtually impossible to perform. Twinning, excessive strains and extreme local variations in the concentration may render the method almost too sensitive to be useful to judge the average variations in concentration from point to point along the scan direction.

Such a pathological case arose in the $\text{Fe}_x\text{Zn}_{1-x}\text{F}_2$ crystals which had been grown by the ACR method discussed in the preceding section. Although these were perfect single crystals, when held up to the light, an array of extremely fine striations in the intensity could be seen with the naked eye. The striations lay in the plane perpendicular to the growth direction. So large and regular were these variations in the index of refraction that, when placed in a HeNe laser beam, a roughly ten-spot diffraction pattern could be projected onto the wall. From the spacing between intensity maxima one could readily determine the "diffraction grating" spacing to be $\sim 100 \mu\text{m}$ and show that it did correspond to the crystal-growth rate multiplied by the ACR cycling period. Unfortunately, the variation of the index was so large that using a wide laser beam and averaging over many striations, the beam was completely depolarized. Since the striations were so fine, one could not make a pinhole small enough to isolate a region of constant birefringence, and hence one could not directly measure either the average concentration variation or the fluctuations in it.

Mixed crystals which were of such poor optical quality that they exhibited very large variations in the concentration gradient were judged to be inappropriate for critical phenomena studies and were not used for these purposes. One exception to this rule was inadvertently

made in critical neutron scattering studies by Birgeneau *et al.*^{15,16} on an $\text{Fe}_{0.5}\text{Zn}_{0.5}\text{F}_2$ crystal grown in our laboratory, but which was not characterized until *after* the neutron measurements had been made. A detailed discussion of this instance is given in the following paper.

V. DISCUSSION AND CONCLUSIONS

The optical birefringence (Δn) technique has been shown to be a powerful method for characterizing the concentration gradient that invariably arises in the growth of two-component (A_xB_{1-x}) single crystals. It is nondestructive and can be performed at ambient temperatures. The primary limitation on its applicability is that it is restricted to systems which are optically anisotropic and transparent and for which some significant difference in Δn exists between the corresponding two pure systems (A and B). The latter restriction is *not* caused by lack of intrinsic sensitivity to the Δn technique but rather comes from the practical limitations on how flat and parallel one can polish opposite faces of a given crystal.

As it has been applied to the $\text{Fe}_x\text{Zn}_{1-x}\text{F}_2$ systems in this paper, the potential of the method has not been fully exploited. Rather than content oneself with exploring just two perpendicular sections as was done above, one could probe an array of closely spaced sections in the two orthogonal directions (Y - Z) perpendicular to the growth axis and, with the aid of a computer, reconstruct a three-dimensional image (computer-assisted tomography) of the concentration profile throughout the crystal. For the purposes to which we have put the method (see following paper¹⁷) the effort required for such an elaboration of the technique would not be justified. But it is quite possible that those interested in the nature of the growth process of mixed crystals would find this sophistication of the method a worthwhile investment. However, even in the present, comparatively simple application of the method is it clear that the Δn technique could be a useful addendum to a crystal-preparation and analysis laboratory.

ACKNOWLEDGMENTS

We are indebted to N. Nighman for having grown all of the crystals used in this study. The research at UCSB has been supported by National Science Foundation Grants No. DMR-80-17582 and No. DMR-85-16786. One of us (D.P.B.) gratefully acknowledges support from the University of California, Santa Cruz, Committee on Research and the Junior Faculty Fellowship Committee.

APPENDIX

The derivation of Eq. (3) proceeds as follows, where the various angles are defined in Fig. 8, and the refractive indices n_1 and n_2 refer to the glass prisms and the sample, respectively. From Snell's law

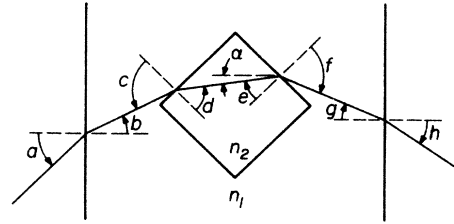


FIG. 8. Refraction of light through a 90° corner of a sample of index n_2 , imbedded in a medium of index n_1 , having plane parallel faces. The angle α is measured with respect to the normal to these faces. The deviation angle is $\theta = a + h$.

$$n_1 \sin c = n_2 \sin d \quad (\text{A1})$$

Using $c = 45^\circ + b$ and $d = 45^\circ + \alpha$, we find

$$n_1 (\sin b + \cos b) = n_2 (\sin \alpha + \cos \alpha) \quad (\text{A2})$$

Using Snell's law again,

$$\sin a + (n_1^2 - \sin^2 a)^{1/2} = n_2 (\sin \alpha + \cos \alpha) \quad (\text{A3})$$

Differentiating with respect to α ,

$$[\cos \alpha - \sin \alpha \cos \alpha (n_1^2 - \sin^2 \alpha)^{-1/2}] da / d\alpha = n_2 (\cos \alpha - \sin \alpha) \quad (\text{A4})$$

Similarly, we find with $e = 45^\circ - \alpha$,

$$[\cosh - \sinh \cosh (n_1^2 - \sin^2 h)^{1/2}] dh / d\alpha = n_2 (-\cos \alpha - \sin \alpha) \quad (\text{A5})$$

Now the total deviation angle $\theta = a + h$, so we add Eqs. (A4) and (A5) to find that

$$\frac{d\theta}{d\alpha} = \frac{d(a+h)}{d\alpha} = 0 \quad (\text{A6})$$

if

$$a = h \quad \text{and} \quad \alpha = 0 \quad (\text{A7})$$

Thus the minimum deviation angle occurs for a symmetric arrangement of incoming and outgoing rays, as in the case of a simple prism. Substituting (A7) into (A3), we see

$$n_2 = \sin(\theta_m / 2) + [n_1^2 - \sin^2(\theta_m / 2)]^{1/2} \quad (\text{A8})$$

where θ_m is the minimum deviation angle.

- ¹D. P. Belanger, A. R. King, and V. Jaccarino, *Phys. Rev. B* **29**, 2636 (1984); D. P. Belanger, Ph.D. thesis, University of California, Santa Barbara, 1981 (unpublished).
- ²D. P. Belanger, A. R. King, V. Jaccarino, and J. L. Cardy, *Phys. Rev. B* **28**, 2522 (1983).
- ³I. B. Ferreira, A. R. King, V. Jaccarino, and J. L. Cardy, *Phys. Rev. B* **28**, 5192 (1982).
- ⁴P. Nordblad, D. P. Belanger, A. R. King, V. Jaccarino, and H. Ikeda, *Phys. Rev. B* **28**, 278 (1983).
- ⁵P. Nordblad, D. P. Belanger, A. R. King, V. Jaccarino, and H. J. Guggenheim, *J. Magn. Magn. Mater.* **31-34**, 1093 (1983).
- ⁶D. P. Belanger, P. Nordblad, A. R. King, V. Jaccarino, L. Lundgren, and O. Beckman, *J. Magn. Magn. Mater.* **31-34**, 1095 (1983).
- ⁷*Introduction to Geometrical and Physical Optics*, edited by Joseph Morgan (McGraw-Hill, New York, 1953).
- ⁸I. R. Jahn, *Phys. Status Solidi B* **57**, 681 (1973).
- ⁹D. Elwell and H. J. Scheel, *Crystal Growth from High Temperature Solutions* (Academic, London, 1975).
- ¹⁰H. J. Scheel, *J. Cryst. Growth* **13-14**, 560 (1972).
- ¹¹This is not a spurious effect caused by polishing thickness variation at edges of the crystal.
- ¹²D. P. Belanger, A. R. King, and V. Jaccarino, *Phys. Rev. B* **34**, 452 (1986).
- ¹³A. R. King, J. A. Mydosh, and V. Jaccarino, *Phys. Rev.* **56**, 2525 (1986).
- ¹⁴C. Magon, J. Sartorelli, A. R. King, V. Jaccarino, M. Itoh, H. Yasuoka, and P. Heller, *J. Magn. Magn. Mater.* **54-57**, 49 (1986).
- ¹⁵R. J. Birgeneau, R. A. Cowley, G. Shirane, H. Yoshizawa, D. P. Belanger, A. R. King, and V. Jaccarino, *Phys. Rev. B* **27**, 6747 (1983).
- ¹⁶R. A. Cowley, H. Yoshizawa, G. Shirane, and R. J. Birgeneau, *Z. Phys. B* **58**, 15 (1984).
- ¹⁷D. P. Belanger, A. R. King, I. B. Ferreira, and V. Jaccarino, following paper, *Phys. Rev. B* **37**, 226 (1988).